Evaluation of dilatometer dissipation test data

E. Imre
Obuda University, BGK and HMB Systems EKIK, Budapest, Hungary, imre.emoke@kvk.uni-obuda.hu

L. Bates L., S. Fityus
University of Newcastle, Newcastle, Australia

M. Hegedus, Zs. Hortobagyi
Budapest University of Technology and Economics, Budapest, Hungary

V. P. Singh
Texas A.&M. University, USA

ABSTRACT: The paper presents the very first steps made to automatically evaluate the total stress dissipation test with a mathematically precise model and inverse solver. Being the DMT and CPT PSL (piezo-lateral stress cell) total stress dissipation tests similar, both PSL test and DMTA total stress data were evaluated. The results indicated that the model error due to the stress release is less for the DMTA data than for CPT PSL data. A new coupled consolidation model family (with oedometric, cylindrical, spherical models) with constant displacement domain is started to be used. The time dependent constitutive law is ensured such that the consolidation model is superimposed with a relaxation model.

Keywords: coupled consolidation, point-symmetric, pore water dissipation, total stress dissipation.

1. Introduction

The total stress dissipation tests have been developed for the assessment of the in situ permeability/c of the soils and the value/time variation of the radial effective stress which is important eg., in pile design and eg., in offshore well constuction. The dissipation tests can not be evaluated at present in a mathematically precise way.

The broader research work is focused on the modelling and evaluation of the following similar tests: (1) oedometric relaxation test, (2) total stress, pore water pressure and effective stress dissipation tests, (3) cone resistance and shaft friction dissipation tests.

For this aim coupled consolidation models were elaborated. These tests are made after partly drained or undrained load imposition. In the oedometer case the displacement domain is the sample, in the penetrometer case the displacement domain is related to the undrained penetration theory of Baligh, initial condition is identified in both cases. Inverse solver was suggested and evaluation method for MRT was validated.

In this paper the results of the first part of the research are applied for the evaluation of the total stress dissipation tests of the CPT and DMT.

1.1. The dissipation tests considered

The laboratory and the in situ (CPTu involved) dissipation tests are shown in Tables 1, 2. In the oedometric relaxation test, the total stress and the pore water pressure are measured, the effective stress is computed.

In the DMTA dissipation test the radial total stress is measured immediately after penetration is stopped in the function of the time (A data).

In the DMTC test the measurement is made after an inflation and a deflation of the membrane, a kind of pore water pressure is measured if the borehole is not moving inwards [1].

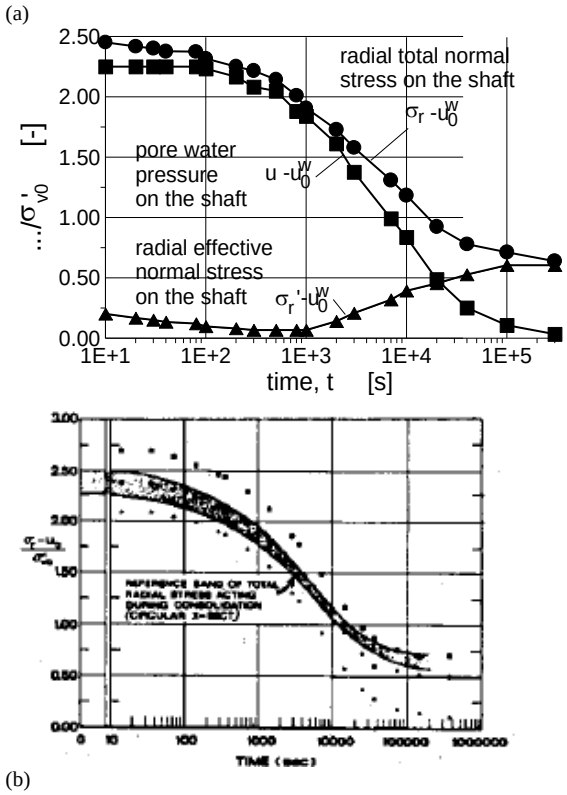

Figure 1. Comparing DMT with the piezo-lateral stress cell test data. (a) and (b) piezo-lateral stress cell test and DMTA data in BBC.

During a CPT piezo-lateral stress PSL cell test, the radial total stress and the pore water pressure are measured, the effective stress is computed. Some important features in a measurement in Boston Blue Clay [2] are (i) the radial total stress at the shaft decreases by 73% of its value valid immediately after penetration, (ii) the radial effective stress is less than the horizontal effective stress 'at rest' immediately after penetration and it further decreases in the first minutes, (iii) the monotonously in-

creases up to the horizontal effective stress 'at rest' before penetration (Fig. 1).

According to strain path models [3,4] the piIe diameter has no influence on the stress at the pile-soil interface at the time of installation. Experimental results [3] show that, in lightly OC Boston Blue Clay, the shape of the penetrating object has minor influence on the data (Fig. 1). The very similar values of the ratios $(\sigma_r\text{-}u_0)/\sigma'_{v0}$ support this idea, for a circular cross section Baligh et al (1985) [2] found for the BBC 2.3 and 2.4, in dilatometer blade the range is 1.8 to 2.5.

1.2. The dissipation test evaluation

No validated model is available, at present, for interpreting the DMTA/CPT total stress or effective stress dissipation curve although the total stress dissipation curves are considerably simpler to obtain than dissipation curves involving the measurement of pore water pressure. Approximate methods are used.

Table 1. Oedometric dissipation tests, constant boundary condition

(Multistage) relaxation test	(MRT)
(Multistage) compression test	(MCT)

Table 2. Types dissipation tests made with penetrometers.

Measured variable	dissipation test made by
Pore water pressure dissipation test, sensor on the shaft and/or on the tip	CPTu (static cone penetrometer)
Total stress dissipation test, sensor on the shaft and/or on the tip	CPTuσ, piezo-lateral stress cell DMTA CPTq_c
Effective stress dissipation test, sensor on the shaft	CPTf_s

Table 3. Point-symmetric uncoupled consolidation model-family

	uncoupled
1-dimensional	Terzaghi (1923) [8]
2-dimensional	Soderberg (1962) [11]
3-dimensional	Torstensson (1975) [14]

Table 4. Point-symmetric coupled 2 consolidation model-family

ε boundary condition	v-ε (coupled 2)
no (uncoupled)	Biot (1941) [10]
v-v (coupled 1)	Randolph at al (1979) [13]
v-ε (coupled 2)	Imre & Rózsa (2005) [15]

Table 5. Point-symmetric coupled 1 consolidation model-family

v boundary condition	v-v (coupled 1)
no (uncoupled)	Imre (1997-1999) [9]
v-v (coupled 1)	Imre & Rózsa (1998) [6]
v-ε (coupled 2)	Imre & Rózsa (2002) [7]

Note: uncoupled-like coupled model, the pore water pressure solution agrees with the uncoupled one ([19], Sills 1975).

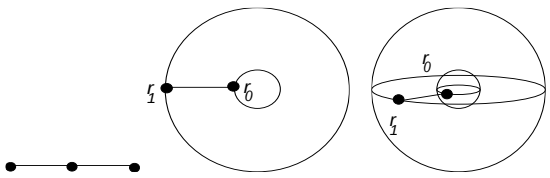

Figure 2. The displacement domain bounded by a (a) 0 dimensional sphere (oedometer model), (b) 1 dimensional sphere (cylindrical model), (c) 2 dimensional sphere (spherical model).

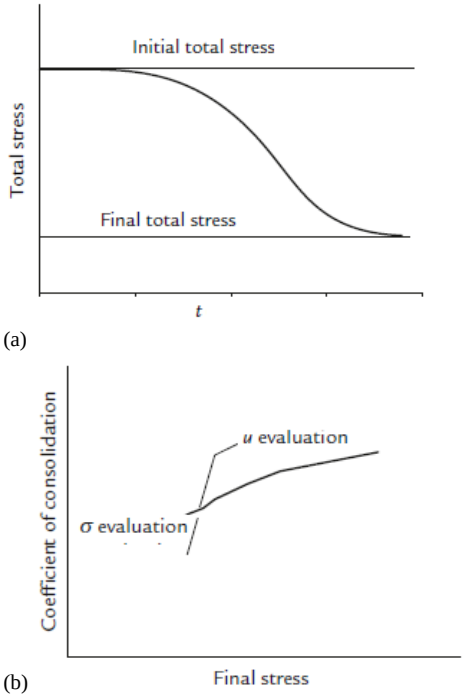

Figure 3. (a) Total stress model with time independent constitutive. (b) Matching of identified c values determined by the Flex method and by the pore water pressure evaluation software from generated u data.

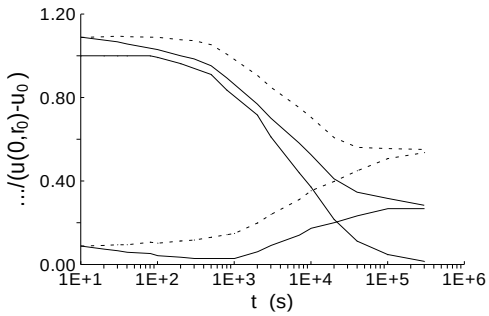

Figure 4. Total stress model-versions. The joined model constructed by the superimposement of a relaxation and a consolidation term (continuous line), coupled 1 consolidation model with time independent constitutive law (dashed line).

1.2.1. The Flex evaluation method

The coefficient of consolidation c is determined with the following one-point fitting equation:

$$c = F\ \mathrm{cm}^2/t_{50} \qquad (1)$$

where F is between 7 and 12, and the t_{50} or t_F is related to the inflexion point of the total stress – time curve. This method does not provide any reliability information and fails if no inflexion point can be separated from the measured total stress data.

The assessment of the inflexion point is generally mathematically not trivial, it is tried to be separated by curve fitting with 3-order parabola in this work (with limited success).

1.2.2. The "matching" evaluation method

In the suggested approximate total stress pile dissipation evaluation method, the total stress and some derived pore water pressure functions are evaluated separately. Repeating the following algorithm for the

measured data set (i=1..N), the final total stress parameter $\sigma_r^s(r_0)_i$ and two values for c are determined. The final total stress parameter $\sigma_r^s(r_0)_i$ - c relations computed for each measuring time value t_i in two ways are matched (Fig 3).

For the first relation, the final stress is computed for each given measuring time value t_i:

$$\sigma_r^s(r_0)_i = 2\sigma(ti) - \sigma_r\ (t=0, r_0), \quad (2)$$

assuming that the total stress value at t_i is the average of the initial and the final total stress, and t_i is the inflexion point. The related c(t_i) is determined by Eq (2) for each t_i (see Fig.3), the $\sigma_r^s(r_0)_i$ – c flex (t_i) is determined.

For the second relation, the mean pore water pressure function is deduced by subtracting the $\sigma_r^s(r_0)_i$ from the measured total stress data and it is approximately transformed into a pore water function (see App.2) which is used to identify a c value, and the c value is represented in terms of the final total stress parameter $\sigma_r^s(r_0)_i$. By determining the c for these u data, the resulting c is given in terms of $\sigma_r^s(r_0)_i$ and is compared with the flex method $\sigma_r^s(r_0)_i$ – c flex (t_i) function.

1.3. The content of the paper

1.3.1. The models tested here

The linear, point-symmetric coupled consolidation models, for every space dimension m (1: oedometer tests, 2: cylindrical and 3: spherical tests) were analyzed in the first part of the research (App 1, [1 to 11].

Three model families are presented in Table 3 to 5. These differ in the boundary condition at r_1, the outer, unknown boundary within the soil, at the zero-pore water pressure line.

For the total stress dissipation modelling, the coupled 1 model family with only displacement type boundary conditions (Table 5) may prognosticate total stress drop only, and a relaxation part-model is needed to be superimposed. Moreover, using the model law, any space dimensional coupled 1 model can be applied. The coupled 2 models and the uncoupled prognosticate constant total stress at the inner boundary (pile shaft).

1.3.2. The aim and content of paper

The aim of this paper to start to model the total stress dissipation after pile penetration. The simplest model-versions were validated (odeometric consolidation and joined model-versions and cylindrical consolidation model-versions) using PSL and DMTA data.

It can be noted that the so defined oedometric model-family was previously validated using oedometer relaxation test data and an automatic the inverse solver with reliability testing methods (also elaborated during the research).

The fitting error was less for the joined model-versions including the relaxation part-model than for the consolidation models alone. The merit function for the joined model was characterized by two minima, only one initial condition (with the larger c value) was physically admissible.

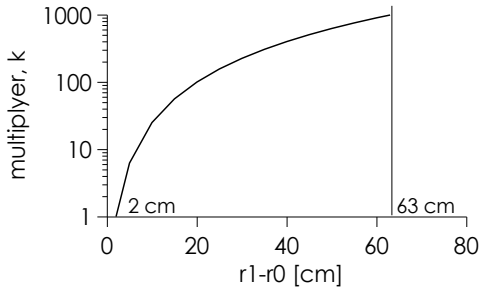

Figure 5. If PSL stress cell test or DMTA data are evaluated with oedometric model with H 2cm, then the identified c is transformed by a multiplier k depending on r_1-r_0.

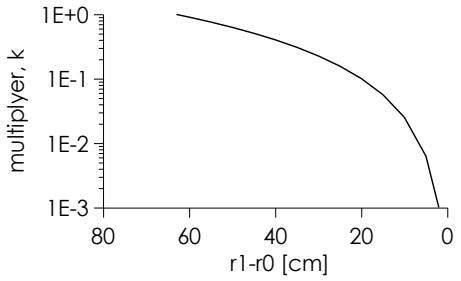

Figure 6. If PSL stress cell test or DMTA data are evaluated with cylindrical model with r_1-r_0=*63*cm (un- drained penetration), then the identified c is transformed by a multiplier k depending on r_1-r_0. if the penetration is partly drained and, therefore, $r_1 < 37r_0$

The previously validated oedometer model-versions were used such that the identified c values were transformed using a model law concerning the size of the displacement domains of the two problems. The model law is following from an approximate time factor concept derived in the first part of the research.

The displacement domain of the penetration problem was assessed from strain path solution assuming that the penetration is undrained. The cylindrical models were used with this assumption, using a displacement domain of r_1-r_0=*63*cm (undrained penetration), where r_1= radius of the zero pore water pressure line, r_0= radius of penetrometer.

The transformation for a different displacement domain is also possible in this case with the same model law, for a smaller r_1-r_0 in case of partly drained penetration.

No correction function was used to compensate the model error due to spring back stress release, this effect is built in the identified initial condition. The approximate evaluation methods were also used, and the results were compared.

2. Methods

2.1. Models

2.1.1. The consolidation models

For the total stress dissipation modelling, only the coupled 1 models with a new, displacement type boundary condition are acceptable. The reason of this that a considerable total stress drop is encountered during the tests and the coupled 2 models prognosticate constant total stress at the shaft.

The structure of the solution was determined using the concept of linear ordinary differential equations [5]. The solution is to a sum for each stress variable:

$$\bullet(t,r) = \bullet^{p}(r) + \bullet^{L}(r) + \bullet^{t}(t,r) + \bullet^{w} \quad (3)$$

where the superscripts *p* or *L* indicate the steady-state, drained continuum-mechanical or seepage problems resp., *t* indicates transient, *w* concerns the self-weight component.

The solutions of the point-symmetric, linear, coupled 1 consolidation model family were suggested for the evaluation of the total stress dissipation tests which have the following features (Fig. 4).

(i) The volume of the displacement domain is unchanged (that follows from the geometric boundary conditions), if the solution is undrained, the final stress state is the same as the initial before penetration.

(ii) Being the volume (and, the mean of the first invariant of the effective stress tensor) constant, the mean of the first invariant of the total stress decreases is in direct proportion with mean pore water pressure.

The key parameter of the models is the initial mean pore water pressure, which equals to the total stress drop due to consolidation and controls the rate of the pore water pressure dissipation.

(iii) The analytical solutions of the coupled 1 consolidation models for *m*= 1, 2 and 3 are very similar, can approximately be interchanged using the approximate time factor concept. The transformation is depending on the r_1= radius of the zero pore water pressure line after penetration.

2.1.2. The joined models

It is assumed that the total normal stress at the measuring interface can be described by a joined model consisting of a linear coupled consolidation part-model and a relaxation part-model which are superimposed:

$$\sigma(t) = \sigma^{c}(t) + \Delta\sigma^{r}(t) \quad (4)$$

where superscripts *c* and *r* indicate the consolidation and, the relaxation part-models, respectively. The relaxation term in here is negative causing stress decrease. Since no relaxation equation is known for the oedometer test/DMT or CPT total stress dissipation test, the following relaxation part-model in case of partial unloading before the dissipation [21] is suggested:

$$\Delta\sigma^{r}(t) = -s\,\sigma(0)\frac{1}{1-s\,b}\log\left[\frac{t+t_1}{t_1+t_3}\right];\; t > t_1+t_3 \quad (5)$$

where s is the coefficient of relaxation, t_1 the delay time, t_3 is the pause of relaxation, b=log((t_1+t_3)/t_1). Value of t_3 and b are zero if no partial unloading takes place, the relaxation term is zero if $t \le t_3$.

The effective stress solutions of the joined model family have the following common feature. The change in the effective stress due to relaxation is negative, due to consolidation is positive. The permeability, the initial mean pore water pressure and the coefficient of relaxation may influence the net time variation of the effective stress significantly. The net interface effective stress variation is different for large and small permeability soils at small and large values of elapsed time.

2.2. Measured data

The evolution of the total stress with respect to time is relatively independent from dimensions and (according to preliminary evidence) shape of the penetrating object. For the model validation, partly PSL cell test data, partly DMT dissipation test data are used from earlier works which are reevaluated. Sometimes total stress and pore water pressure data are evaluated together, sometimes separately, these cases are indicated.

2.3. Model fitting, model-versions

Both the oedometric relaxation test model and the cylindrical evaluation model – consisting of a point-symmetric, linear, coupled 1 consolidation model and an empirical relaxation part-model in the most complex case – was used for the evaluation of DMT and CPTu total stress dissipation tests.

In the algorithm (App 3), the implicit function theorem was used to split the parameter vector (1st group: linearly dependent parameters, 2nd group: non-linearly dependent parameters) and the minimization was split into two, lower-dimensional steps, a linear one and a nonlinear one.

The linearly dependent parameters were identified separately for fixed values of the non-linearly dependent parameters, situated in the points of a parameter grid. In the nonlinear minimization, the solution was bracketed by computing the merit function in the points of the foregoing non-linear parameter grid, assuming convex level lines.

Using the computation, the deepest 1d sensitivity sections ('clever sections') of the merit function for the 2nd type parameters were determined and used for reliability testing**.** Since the computer time depends exponentially on the number of the 2nd group parameters, reduced model-versions were made as follows.

2.3.1. Oedometer model-versions

The analytical solution of coupled consolidation model for the total stress σ and the pore water pressure *u* (see App 1):

$$\sigma(t) = -\sum_{i=1}^{\infty}\varphi_i\, e^{-i^2\pi^2 T} + \sigma_\infty - \Delta\sigma^{r}(t) \quad (6)$$

$$u(t,y) = -\sum_{i=1}^{\infty}\varphi_i[\cos(y(i\,\pi/H) - 1]\; e^{-i^2\pi^2 T} \quad (7)$$

where σ_∞ is the asymptotic total stress, *t* is time, *y* is distance, $T = ct/H^2$ is the time factor, c is the coefficient of consolidation, ϕ_i are Fourier coefficients related to the initial condition shape function:

$$u(0,y) = A\; y^3 + B\;\; y^2 + C\;\; y \quad (8)$$

A, B and C are initial condition parameters. The analytical solution of joined model for total stress:

$$\sigma(t) = -\sum_{i=1}^{\infty}\varphi_i\, e^{-i^2\pi^2 T} + \sigma_\infty - \Delta\sigma^{r}(t) \quad (9)$$

The solution contains 7 parameters, 3 out them are with non-linear dependence (Tables 6, 7). In model-version HCRT parameter t_1 is specified, and, a minor

change is made in the relaxation parameter modelling. The product of s and $\sigma(0)$ denoted by s_k

$$s_k = s\ \sigma(0) \quad (10)$$

is identified. The term $\sigma(0)$ can be expressed as the linear combination of other parameters:

$$\sigma(0) = \sigma_\infty + D \quad (11)$$

where D is the mean initial pore water pressure. The solution depends linearly on s_k. The number of the non-linearly dependent parameters was decreased to 2 and, the computational work was less by two orders of magnitude than the one for model H (Table 6). In model-version HCR only one parameter of the relaxation part-model is identified (s_k), t_3 is zero. No relaxation is modeled in model-version HC. The number of the non-linearly dependent parameters is 1 for these.

It can be noted that parameters σ_∞ and c have different meaning if relaxation is modelled or is not. For model-versions H, HCRT, HCR the compression curve constructed from the identified σ_∞ is time independent, while the identified σ_∞ is time dependent, depending on the stage duration for model-version HC.

2.3.2. Oedometer solution for piles

The model law applies if the pile problem is solved with the oedometric relaxation test model, the solution is transfomed using the the time factor as follows:

$$\frac{c_1}{H^2} = \frac{c_2}{(r_1 - r_o)^2},\ c_2 = (r_1 - r_o)^2 \frac{c_1}{H^2} = k c_1 \quad (12)$$

$$T = \frac{ct}{(r_1 - r_o)^2} \quad (13)$$

Assuming that $T_1 = T_2$, $t_1 = t_2$, sample height H=2cm, to a domain $r_1 = 37 r_0$, r_0= 1,75 cm, r_1-r_0=63cm (undrained penetration), a multiplier k=63*63/4 can be derived for the c values. For partly drained penetration, the position of the zero pore water pressure line is $r_1 < 37 r_0$ and constant multiplier can be computed with eq 12.

2.3.3. Cylindrical model-versions

The solution of the coupled 1 cylindrical consolidation model for the pore water pressure (u) and radial total stress in the cylindrical case has the same terms as in eq 6,7, only the form is changing from sin and cosine to the Bessel functions:

$$u = \sum_{k=0}^{\infty} \lambda_k C_k e^{-\gamma_k^2 \cdot c_h \cdot t} \begin{Bmatrix} [I_0(\lambda_k r) + \mu_k Y_0(\lambda_k r)] \\ -[I_0(\lambda_k r_1) + \mu_k Y_0(\lambda_k r_1)] \end{Bmatrix} \quad (14)$$

$$\sigma^t = \sum_{k=0}^{\infty} \lambda_k C_k e^{-\gamma_k^2 \cdot c_h \cdot t} \left\{ -[I_0(\lambda_k r_1) + \mu_k Y_0(\lambda_k r_1)] \right\} \quad (15)$$

where J_p and Y_p are the Bessel functions of the first and second kind, of order p, λ_k, μ_k are the roots of the boundary condition equations (depending on r_1 and r_0); C_k (k=1.∞) are the Bessel coefficients determinable from the initial condition, and c is coefficient of consolidation ($c = k\, E_{oed}/\gamma_v$).

The identified parameters of the various model-versions were as follows. In pore water pressure and total stress models 1a the linearly dependent initial condition parameters C_k (k=1.n) were directly identified during the inverse problem solution. The numerical work was the same as for model HC, the related evaluation method is called as fast (Table 7).

In the analytical solution of total stress there is a constant for the steady-state part of the solution and a log part of the solution for the relaxation term (eq 6). It means that this is a function 1 and log t in the linear part of which we are looking for coefficients. Three codes were made, with and without the constant term (the latter solution was numerically more stable) and one with two additional terms. Since the functions 1 and log t are linearly independent, slightly different results are encountered. In this work the codes with consolidation modelling were used only.

In the pore water pressure model 1b the C_k (k=1.250) were determined beforehand for various monotonic or non-monotonic shape functions, with three additional non-linearly dependent parameters, giving a more precise solution. The numerical work is the same as in the case of model H (Table 7), the evaluation method is slow. (The shape functions may contain a negative part due to the interface shear in a thin zone along the shaft and a positive part due to the penetration normal stresses. Hence, 350 shape functions (and to negative scaling, 350 mirror image shape functions) are used.)

Table 6. Parameters of the most general oedometric model-version H

Parameter	Symbol	Dependence
initial condition	A, B , C	linear
Coeff. of consolidation	c	nonlinear
asymptotic total stress	σ_∞	linear
coefficient of relaxation	s	nonlinear
pause of relaxation	t_3	nonlinear
delay time	t_1	nonlinear

Table 7. Computational effort for the versions of model H

Model-version	Identified parameters	Function value evaluations
H	A, B, C, c*, σ_∞, s*, t_3*	~10E4
HCRT	A, B, C, c*, σ_∞, s_k, t_3*	~10E3
HCR	A, B, C, c*, σ_∞, s_k	~10E2
HC	A, B, C, c*, σ_∞	~10E2

• nonlinearly dependent

Table 8. Evaluation of the PSL test. The identified parameters for the total stress: c, final total stress σ_∞ and coefficient of relaxation s, for pore water pressure: c. (c multiplier k=63*63/4)

Model-version	c [cm2/s]	s [-]	σ_∞ [-]
HC consolidation model σ,u	1,98E-02		0.28
HCR joined model σ,u	2,48E-02	0.04	0.37
HCRT joined model σ,u	2,48E-02	0,04	0.4
Cylindrical consolidation 1a, σ	2.00E-02		
Cylindrical consolidation 1a, u	2.00E-02		
Cylindrical consolidation 1b, u	9.00E-03		

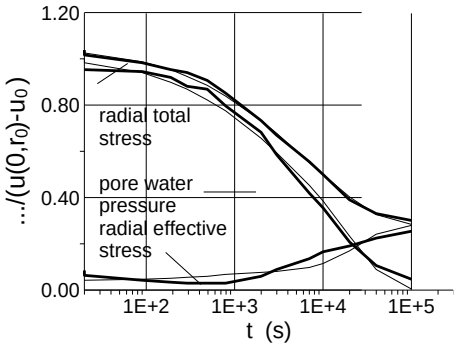

Figure 7. Evaluation of the PSL cell test data with the HC model.

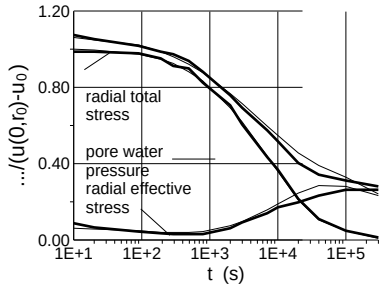

Figure 8. Evaluation of the PSL cell test data with the HCR model.

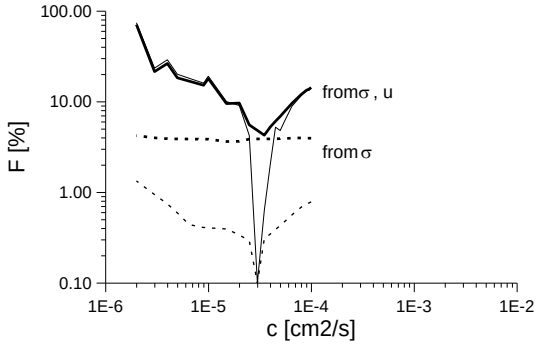

Figure 9. The deepest sensitivity sections of the merit function concerning parameter *c*. Evaluation of the PSL test total stress and pore water pressure data with the HC model. The solution determined from total stress data only is shown in dashed line. The c value is uncorrected, the corrected *c* is indicated in the Tables.

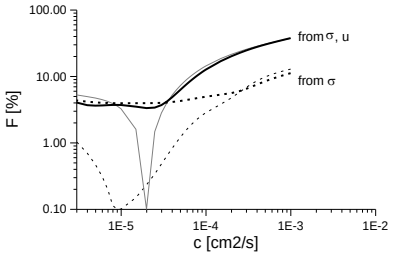

Figure 10. The deepest sensitivity sections of the merit function concerning parameter *c*. Evaluation of the PSL total stress and pore water pressure data with the HCRT model. The solution determined from total stress data only shown in dashed line. The *c* value is uncorrected, the corrected *c* is indicated in the Tables.

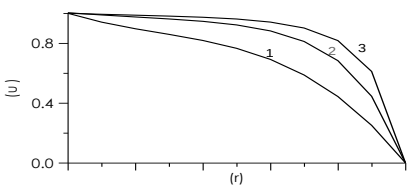

Figure 11. Evaluation of the PSL cell test data test data. Identified initial condition 1:HCR, 2:HC, 3: HCRT, the mean pore water pressure is larger than expected.

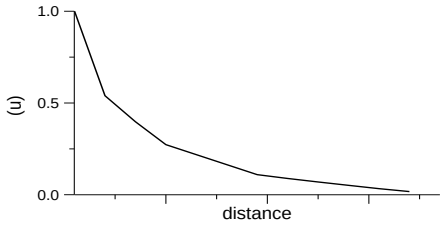

Figure 12. Expected initial condition (solution of undrained penetration problem, Baligh 1986[4])

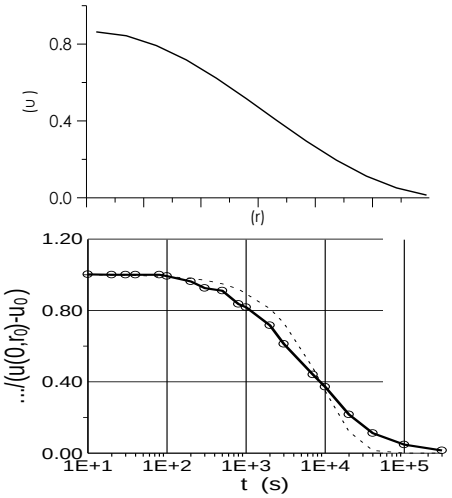

Figure 13. The piezo-lateral stress cell, pore water pressure data evaluation with cylindrical model 1a, 'fast method' (a) identified initial condition, (b) fitted and measured data.

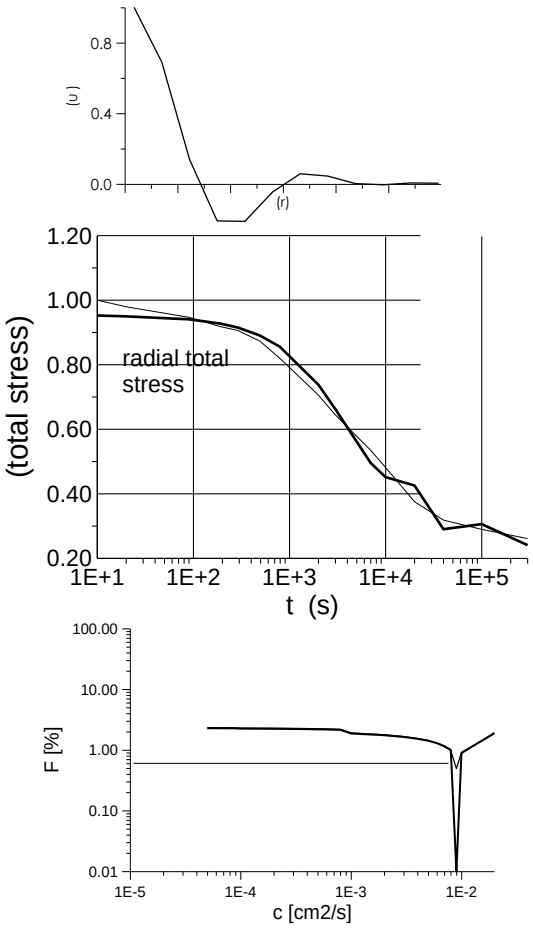

Figure 14. The PSL cell total stress data evaluation with cylindrical model 1a, 'fast method' (a) identified initial condition, (b) fitted and measured data, (c) unique solution and error range.

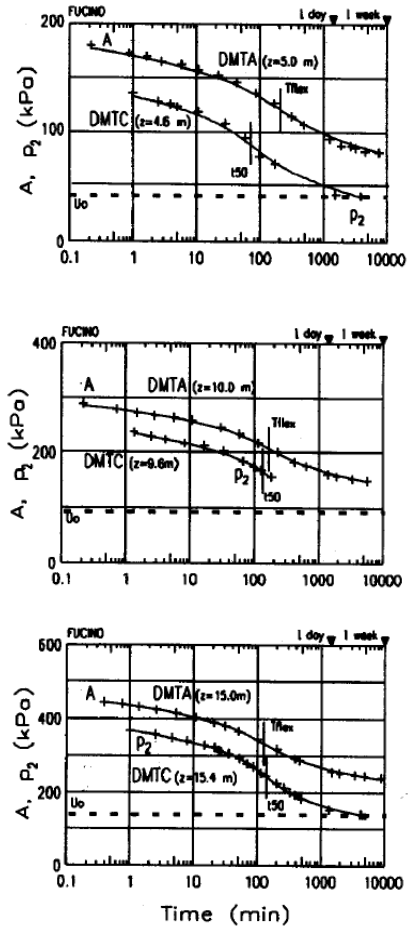

Figure 15. Fucino DMTA and DMTB data measured at 5m. 10m, 15m (from Totani et al, 1998).

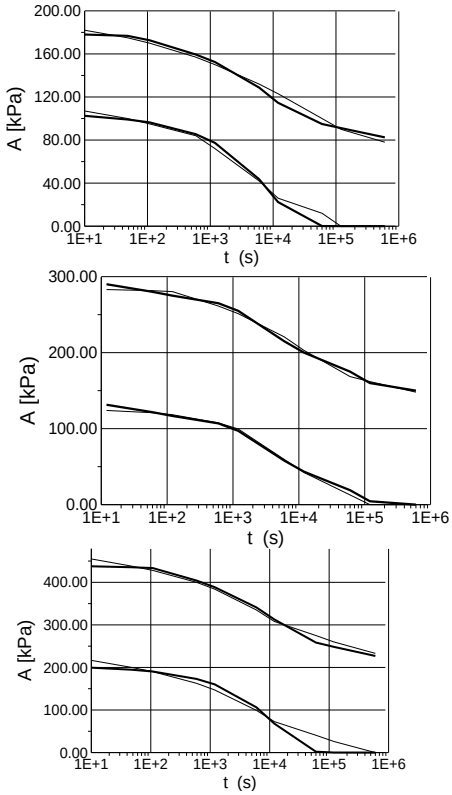

Figure 16. Fucino DMTA data evaluated together with u data generated with match method and Model HCRT, a to c: fitted and measured data at 5m. 10m, 15m, resp. [1].

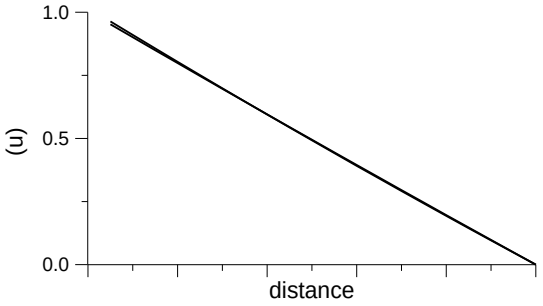

Figure 17. Fucino DMTA data evaluated together with u data generated with match method and Model HCRT, initial condition identified, a to c: at 5m. 10m, 15m, resp. [1].

3. Results – PLS data

3.1. Oedometer models

When the measured data used were total stress (pore water pressure and, therefore, effective stress), the results (identified parameters and initial conditions, fitted and measured data) are shown in Table 8, Figs 5 to 10.

According to the results, the solution of the inverse problem was reliable if pore water pressure data were simultaneously fitted, but the initial condition identified was differing from the shape expected.

Evaluating total stress only with the oedometer model, the results showed that the inverse problem became ill-conditioned. The deepest sensitivity section, in Figures 7 and 8 (without and with relaxation modelling) indicates non-well-defined global minimum.

The HC simulated effective stress (thin) is monotonically increasing with time since no relaxation is modeled. The HCR simulated effective stress (thin) is non-monotonic with relaxation modeling.

3.2. Cylindrical models

The cylindrical models 1a and 1b, gave coefficient of consolidation of 2 E-02 cm^2/s 9 E-03 cm^2/s resp for pore water pressure. The identified initial condition is realistic (Table 8, Figs 13, 14). Similar results were found for the total stress data with model 1a.

4. Results – DMT data

4.1. Oedometer models

Evaluating DMTA and pore water pressure data together, the results are shown in Figures 15 to 18, Table 9, 10. (The pore water pressure data were generated with the matching method (see App.2)).

The inverse problem was well conditioned. Using consolidation model HC, due to the double model differences (m=1<2 model, no relaxation), the identified *c* values were smaller with a factor of about 5 than the values for the HCRT model. These values were transformed (c multiplier k=63*63/4).

Evaluating DMTA total stress alone, results are shown in Tables 11 to 15, Figs. 17 to 23. Using the oedometric model HC, HCR, the inverse problem solution was reliable. The inverse problem solution was with less error for HC than HCR.

The identified *c* values for models HCR or HC were smaller by one or half order of magnitude than the ones of the HCRT model using total stress and generated pore water pressure data.

The oedometer models gave larger initial mean pore water pressure than expected due to total stress release of the equipment. The identified initial conditions for the two types total stress data differed, reflecting larger stress release for the piezo-lateral stress cell test data than for DMT data.

Table 9. Model HC results for the coefficient of consolidation c [cm^2/s], with confidence interval, using Fucino DMTA data and generated matching method u data at 5m. 10m, 15m.

	c	cmin	cmax
Fucino 5	3,0E-06	1.0E-06	1,0E-05
Fucino 10	6,0E-06	3,0E-06	1,0E-05
Fucino 15	6,0E-06	2,0E-06	1,5E-05

Table 10. Fucino site, model HCRT, 2 "measured data" ("DMTA and generated u), identified c with confidence interval. (*c* multiplier *k*=63*63/4)

	c	c_{min}	c_{max}
Fucino 5m	4,47E-02	2,48E-02	7,44E-02
Fucino 10m	2,98E-02	1,49E-02	4,47E-02
Fucino 15m	2,98E-02	1,49E-02	4,96E-02

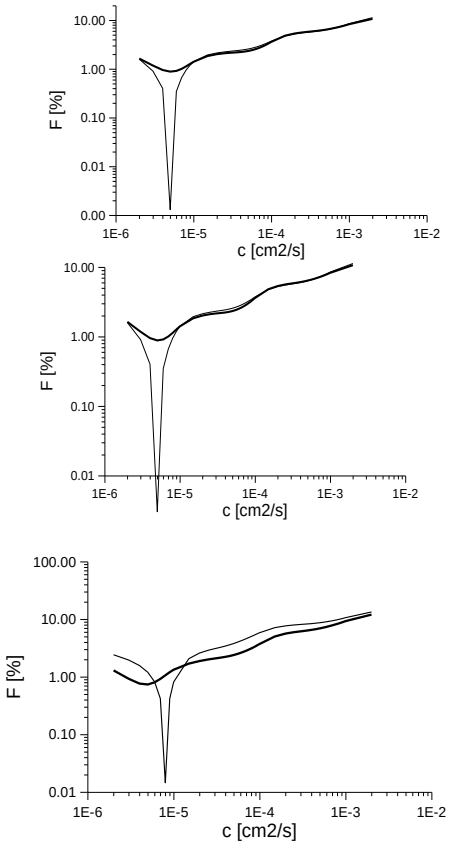

Figure 18. Minimal section, model HC, Fucino DMT dat Totani et al, 1998 [1]). The solution is determined from total stress data. The c value is uncorrected, the corrected *c* is indicated in the Tables.

Table 11. Model HC, DMTA total stress data (Fucino, Newcastle and Ballina sites), *c* [cm^2/s] with confidence interval. (*c* multiplier *k*=63*63/4)

	c	c_{max}	c_{min}
Fucino 5	7,94E-03	9,92E-03	5,95E-03
Fucino 10	4,96E-03	9,92E-03	5,95E-03
Fucino 15	4,96E-03	6,95E-03	3,97E-03
1,5 m	3,97E-01	4,56E-01	3,57E-01
2,5 m	7,94E-01	9,92E-01	6,55E-01
Ballina	9,53E-02	9,92E-02	5,56E-02

Table 12. Model HCR, DMTA total stress data (Fucino, Newcastle and Ballina sites), *c* [cm^2/s] with confidence interval. (*c* multiplier *k*=63*63/4)

	c	c_{min}	c_{max}
Fucino 5	1,49E-02	9,92E-03	5,95E-03
Fucino 10	4,96E-03	9,92E-03	5,95E-03
Fucino 15	8,93E-02	6,95E-03	5,95E-03
1,5 m	4,47E-01	4,56E-01	3,57E-01
2,5 m	9,92E-01	9,92E-01	6,55E-01
Ballina	1,98E-01	9,92E-02	5,56E-02

Table 13. Cylindrical model DMTA total stress data (Fucino, Newcastle and Ballina sites), identified *c* [cm2/s]

	c	c_{min}	c_{max}
Fucino 5	8,0E-3	1,0E-3	6,0E-4
Fucino 10	8,0E-3	1,0E-3	6,0E-4
Fucino 15	9,0E-3	2,0E-3	6,0E-4
1,5 m	4,0E-1	2,60E-1	5,60E-2
2,5 m	6,0E-1	6,0E-1	1,60E-2
Ballina	7,0E-2	9,0E-3	1,60E-3

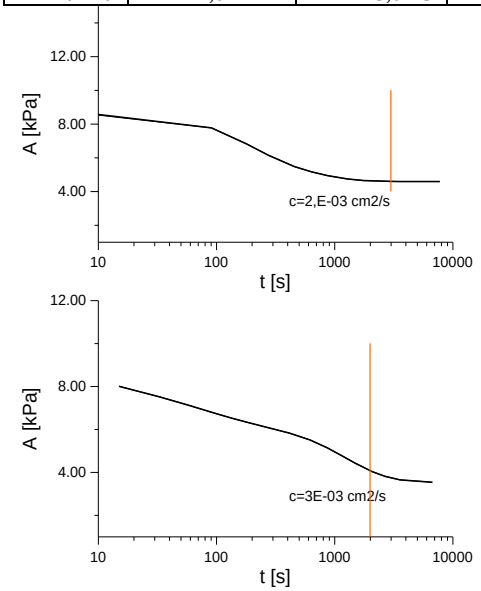

Figure 19. Newcastle DMTA data and fitted 3-order parabola, inflexion point indicated (a) 1.5 m. (b) 2.5 m.

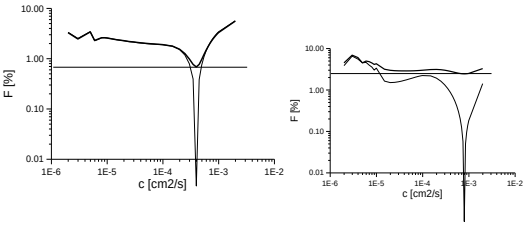

Figure 20. Minimal section, model HC, evaluation of the Newcastle DMT data (a) 1.5 m. (b) 2.5 m. The solution is determined from total stress data, the c value is uncorrected, the precise c indicated in Tables 11, 12 and 14.

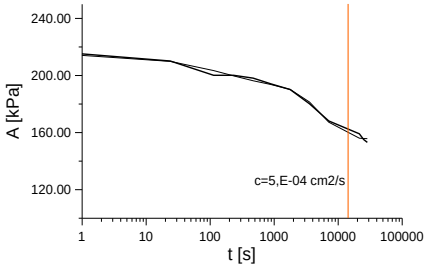

Figure 21. Ballina DMTA data and fitted 3-order parabola, inflexion point indicated.

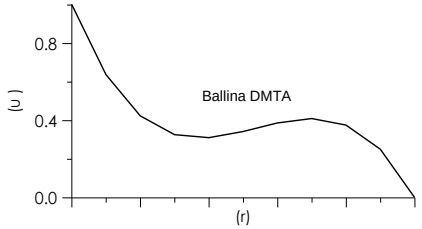

Figure 22. Model HCR, identified initial condition for using Ballina DMTA data.

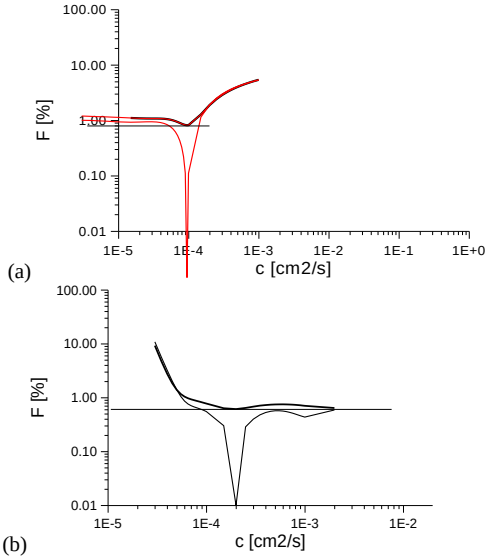

Figure 23. Merit function minimal section, Model HC and HCR, resp., Ballina DMTA data. The c value is uncorrected, the precise c indicated in Tables 11, 12 and 14.

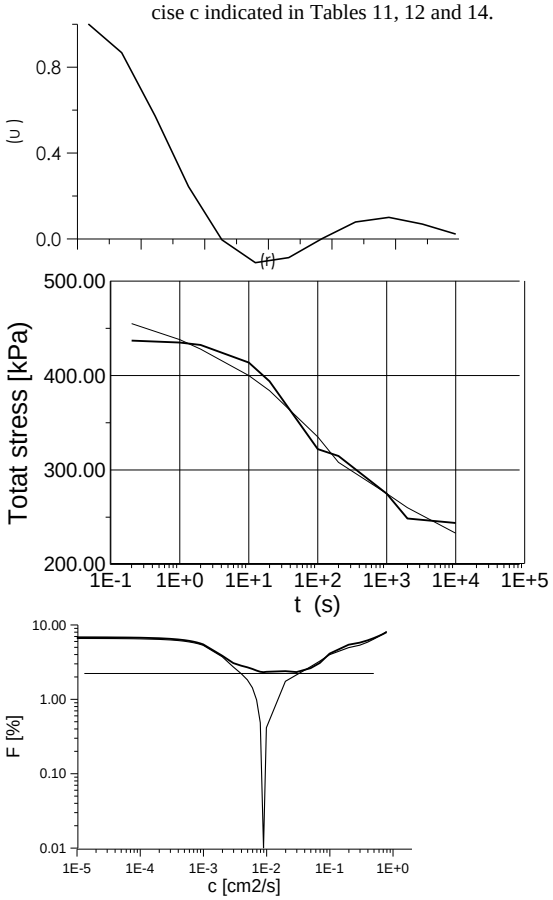

Figure 24. DMT Fucino 3 total stress data evaluation with cylindrical model 1a, 'fast method' (a) identified initial condition, (b) deepest section of merit function.

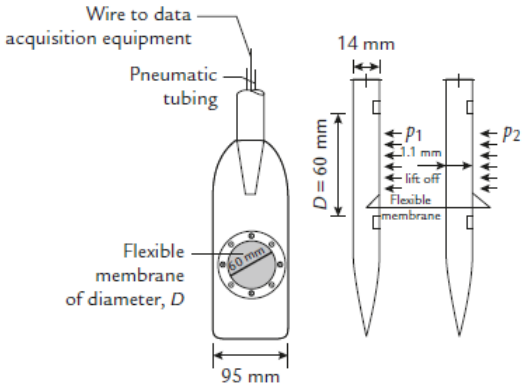

Figure 25. Geometry of DMT.

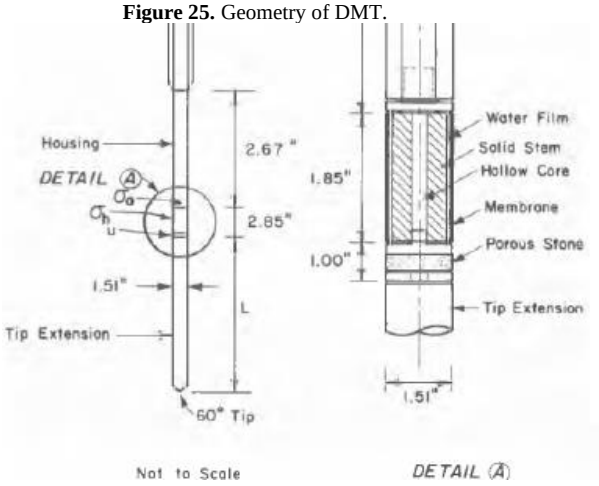

Figure 26. Geometry of the piezo-lateral stress cell.

Figure 27. The DMT tip.

4.2. Cylindrical models

Using cylindrical model, the identified c was larger than the previous values and the lab test results, being in agreement with the earlier DMTA evaluation.

4.3. Identified initial condition

In the lack of a correction factor function for the total stress release of the equipment, the oedometer models gave larger initial mean pore water pressure than expected (see Figs. 9, 10, 16).

Moreover, the identified initial conditions for the two types total stress data differed, reflecting larger

stress release for the piezo-lateral stress cell test data than for DMT data.

The initial conditions identified from PSL pore water pressure data with the cylindrical model 1b using shape functions was physically acceptable. The initial condition identified from exclusively total stress with the fast cylindrical model-versions 1a are approximate but were basically correct (Figs. 14, 24).

4 Discussion

4.1 Rigidity of equipment, stress release

During the dissipation test, stress release due to dissipation takes place, the penetrometers springs back, the spring back displacement is increasing with increasing distance above the tip.

The DMT measurement is made on the tip, on a thin and rigid element, the r_d diameter above it of 1.2 cm (Figs. 25, 27).

A fundamental aspect in the design of the PLS cell is the rigidity (Fig. 26). In the case of the pore pressure measuring device, the fact that a finite amount of water is exchanged between the soil and the sensing element constitutes interference. Such interference can be reduced if the flexibility, or amount of required water exchange, is reduced to a minimum. Similarly, in measuring the total horizontal stress, it is important that the deformation of the measuring system be negligible. Rigidity is ensured by having a solid steel core and only a thin internal water film to which the externally applied pressure is transmitted. The resolution of the CPT in delineating layers is related to the size of the cone tip, with typical cone tips having a cross sectional area of 10 cm², corresponding to diameter of 3.6 cm (>1.2 cm).

Being both equipments rigid, the controlling parameter is the distance of the sensor above the tip in the spring back period. The DMT measurement is made on the tip, on a thin and rigid element. the CPT measurement is made well above the tip on the rod where there is a more pronounced effect of the stress release (Fig. 26). The stress release is therefore more important for the PSL measurement.

The effect of stress release is can be seen from the piezo-lateral stress cell test measurement (Fig. 1a) as follows: the measured and the computed total stress decrease using the theoretical initial condition are different. In detail, the consolidation stress drop is not larger than the initial mean pore water pressure approximated from a linear function, $0.33u(0,r_0) < 0.33\sigma(0,r_0)$, the relaxation stress drop is less than around 0.25 $\sigma(0,r_0)$, the sum is about 0.58 $\sigma(0,r_0)$, being less than the measured 0.75 $\sigma(0,r_0)$.

4.4. Model validation results

4.4.1. Inverse problem solution

In this work, using CPTu PSL and DMT total stress dissipation test data, the merit function was generally characterized by one minimum. In case of total stress data evaluation only, the minimum was nearly degenerated for the PSL data, was nice for DMTA data. This can be interpreted such that (i) since the PSL data have possibly larger stress release effect than DMT data, they gave less reliable solution, and since the oedometric model are less precise than the better cylindrical model, they gave less reliable solution.

4.4.2. Identified initial condition

The effect of spring back release of the equipment is an additional total stress drop, which is increasing with the spring back displacement.

Table 14. Summary of *c* results of DMTA total stress data [cm²/s] (*c* multiplier *k*=63*63/4)

	HC	HCR	cflex	Cylindrical
Fucino 5	7,94E-03	1,49E-02	6,0E-5	1,0E-2
Fucino 10	4,96E-03	4,96E-03	6,0E-5	8,0E-3
Fucino 15	4,96E-03	8,93E-02	6,0E-5	9,0E-3
1,5 m	3,97E-01	4,47E-01	2,0E-3	4,0E-1
2,5 m	7,94E-01	9,92E-01	3,0E-3	6,0E-1
Ballina	9,53E-02	1,98E-01	5,0E-4	7,0E-2

Table 15. Fucino, summary of *c* results of DMTA total stress and generated *u* data (*c* multiplier *k*=63*63/4) made for Figure 28.

model	HC	HCR	cylindrical	HCRT with *u*
5m	7,94E-03	1,49E-02	1,0E-2	4,47E-02
10m	4,96E-03	4,96E-03	8,0E-3	2,98E-02
15m	4,96E-03	8,93E-02	9,0E-3	2,98E-02

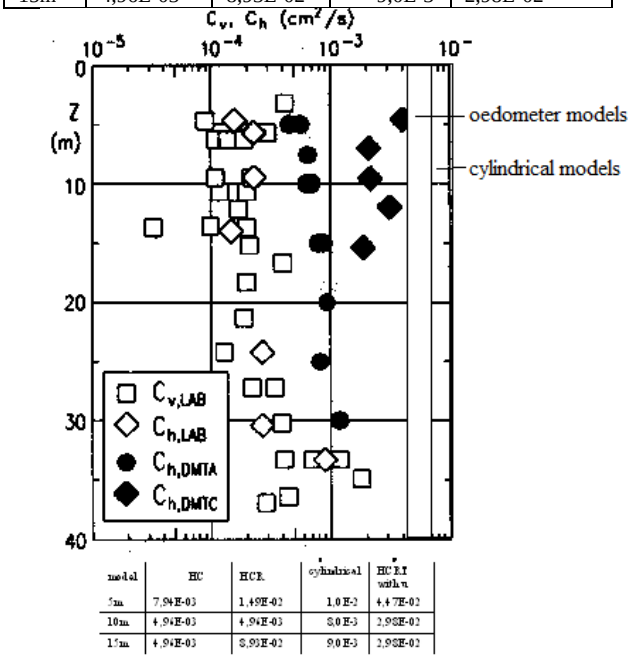

Figure 28. Some identified *c* values from this work, Fucinon site. Note: after applying the model law ((c multiplier k=63*63/4)), the c values for all oedometer and cylindrical model-versions fell in the right blank strips, 1E-2>c>4E-3cm²/s, being the oedometer values slightly smaller.

In the initial condition identified by oedometer models from PSL data, the initial mean pore water pressure was much larger than expected one to give the additional total stress drop (see Figs. 9, 10, 16).

The identified initial conditions differed for the two types of data, reflecting larger stress drop in the case of the PSL cell test data than for DMT data. This follows from the measuring element position. For the well-above the tip position, the identified initial condition from the expected one is a measure of the goodness of

the test with respect to the model assumptions at the total stress evaluation.

The initial conditions identified from exclusively pore water pressure data with the cylindrical models were physically acceptable and was more for the slow than the fast version since in the first case the initial shape functions were used (Fig. 11).

4.1.1 Identified c

Concerning the *c* identified with oedometer models, for the piezo-lateral stress cell test data, the *c* value was less dependent on the oedometer model-versions.

For real DMTA data, the identified *c* value was more dependent on the type of the oedometer model-version. This indicates also that the DMT data are better than PSL data.

All models gave surprisingly large but realistic *c* values (Fig. 28), in the order of magnitude of the previous DMT evaluations, being larger than the previous values.

The identified *c* was slightly smaller for the oedometer models since the drainage surface area is larger for the cylindrical than for the oedometer model.

5. Summary, conclusion

In this paper some mathematically precise models were started to be used to evaluate the total stress (CPT and DMT) dissipation test data, a more approximate oedometer model family and a less approximate cylindrical model.

5.1. The piezo-lateral stress cell test data

1. The same identified *c* value was approximately encountered when the various oedometric relaxation test model-versions (m=1) were fitted on PSL total stress, effective stress and pore water pressure data, possibly due to the large error due to the stress release.

2. The inverse problem was generally ill-conditioned when only PSL total stress data was evaluated with various versions of the oedometer model (the minimum became quasi-degenerated).

3. When cylindrical consolidation model 1a was fitted on pore water pressure or total stress dissipation data then the identified c was practically the same, inverse problem solution was reliable. After applying the model law (*c* multiplier), the oedoemeter *c* data were similar.

5.2. The DMTA data

The first result of six data sets (3 Fucino, 2 Newcastle, 1 Ballina) evaluated with oedometer model or the simplest cylindrical model were as follows.

a) Evaluating DMTA total stress and pore water pressure data together with oedometer models, the inverse problem was generally well conditioned, with unique solution and error range.

b) Evaluating DMTA total stress with oedometer model or the simplest cylindrical model, the inverse problem solution was generally reliable. The identified c values differed in a factor of about 5 to 15 for the various oedometer models.

c) Concerning the well-documented Fucino site and the various oedometer models, after applying the model law (*c* multiplayer), all *c* data fell in the strips 1E-2> c>4E-3cm^2/s, larger than the previous lab test and flex results, being possibly in agreement with the earlier DMTC evaluation and to the actual cylindrical model c value. It can be noted that all results depend on r1.

d) Concerning the well-documented Fucino site and the approximate methods, the inflexion point and the result of the Flex method was not unique. By fitting a 3rd order parabola, the inflexion point differed from the "eye" solution. The Flex method c was therefore in an interval of lab values *c*. The cylindrical model c value was slightly larger than match *c* value (see App 2).

5.3. Conclusions

The DMT or CPT total stress dissipation tests are not evaluated precisely at present, only approximate methods are known. In this work 3 kinds of oedometer models and some simplest possible cylindrical model-versions were started to be tested with CPT PSL stress cell test data and with DMTA total stress dissipation and deduced pore water pressure data. The results were as follows.

1) Concerning the PSL cell test data, the identified c was not too sensitive to the differences in the various oedometric model-versions while concerning the DMT data, the identified c was sensitive to the differences in the various oedometric model-versions

2) Using DMTA total stress data and joined oedemeter model-versions, the inverse problem solution was generally well-conditioned while this was not true when PSL total stress data was used with joined oedometer model-versions. The PSL solution was reliable with joined oedometer model-version when both total stress and u data were used.

3) The inverse problem solution was reliable for the simple cylindrical models, irrespective of the type of the data.

4) The identified initial conditions differed for the CPT and DMT data, reflecting larger stress release and spring back effect for the piezo-lateral stress cell test data than for DMTA data, in accordance with the altitude of the sensor element. In other words, the constant displacement load boundary condition is more approximate for the CPT PSL than for the DMT total stress dissipation test data, the model error is larger for the CPT PSL cell test. The pore water pressure data are not sensitive to this effect.

5)The identified *c* can be characterized as follows for the well-documented Fucino site. After applying the model law (*c* multiplier), all oedometer c data fell in the strip 1E-2> c>4E-3cm^2/s, larger than the previous lab test and flex results, being basically in agreement with the earlier DMTC evaluation and with the actual cylindrical model c values. It can be noted that all results depend on *r1*.

It can be concluded that all models gave surprisingly large but realistic c values, in the order of magnitude of the previous DMT evaluations, being larger than the previous values.

(The identified c is slightly smaller for the oedometer models since the drainage surface area is larger for the cylindrical than for the oedometer model).

The simplest possible cylindrical model (time independent constitutive law, "fast" evaluation method, model 1a) can automatically be used for the evaluation of the DMTA dissipation test data.

In further research, the m=2 (cylindrical) total stress models with initial condition shape functions ("slow" evaluation method) and with time dependent constitutive law will be tested on DMTA total stress data.

In addition, truncated measured data series will be tested to decide whether it is worthy to be used simultaneously with the measurement.

6. References

[1] Totani, G; Clabrese, M; and Monaco, P. In situ determination of ch by flat plate dilatometer. Proceedings of ISC-1, Atlanta, Georgia, 1998. 883–888.

[2] Baligh, M. M.; Martin, R. T.; Azzouz, A. S.& Morrisson, M. J. The piezo-lateral stress cell. Proc. of the 11th ICSMFE San Francisco. 1985. 2:841-844.

[3] Marchetti, S. Totani, G. Campanella, R. G. Robertson, P. K. Taddei, B. "The DMT□ □hc Method for Piles Driven In Clay", Proceedings of In Situ '86. GT. Div. ASCE, June 23-23, 1986 Blacksburg. VA. 765-779.

[4] Baligh M. M. (1984) , "PersonaI Cornmunication to M. Jamiolkowski, also reproduced as Fig. 39 in Jamiolkowski,M. , Ladd C. C, , Germaine,J.T. and Lancellotta,R., New Developments In Field and Laboratory Testing,SOA Report,XI.

[5] Burns, S.E., Mayne, P.W. Coefficient of consolidation ch from type 2 piezocone dissipation test in overconsolidated clay. Proc. of Int.Symp. on CPT. 1995. 137-142.

[6] Imre, E. and Rózsa, P. Consolidation around piles. Proc. of 3rd Sem. on Deep Found. on Bored and Auger Piles. Ghent 1998. 385-391.

[7] Imre, E. and Rózsa, P. Modelling for consolidation around the pile tip. Proc. of the 9th Int. Conf. on Piling and Deep Foundations DFI, Nizza. 2002. 513-519

[8] Terzaghi, K. Theoretical Soil Mechanics. Wiley: New York, 1948. 1-510.

[9] Imre, E. Consolidation models for the incremental oedometric tests. Acta Technica Acad. Sci. Hung. 1997-1999. 369-398.

[10] Biot, M. A. Theory of elasticity and consolidation for porous anisotropic solid. Jl. of Appl. Phys. 1955. 26:182-185.

[11] Soderberg, L. O Consolidation Theory Applied to Foundation Pile Time Effects. Geotechnique, 1962.12. 217-232.

[12] Imre, E. & Rózsa, P. Consolidation around piles. Proc. of 3rd Seminar on Deep Foundations on Bored and Auger Piles. Ghent 1998. 385-391

[13] Randolph, M. F. & Wroth, C. P An analytical solution for the consolidation around displacement piles. I. J. for Num. Anal. Meth. in Geomechanics, 1979 3:217-229.

[14] Torstensson, B. A. The pore pressure probe. 1977. Paper No. 34. NGI

[15] Imre, E. and Rózsa, P. Modelling for consolidation around the pile tip. Proc. of the 9th Int. Conf. on Piling and Deep Foundations DFI, Nizza. 2002. 513-519

[16] Imre E, Rozsa P, Bates L, Fityus S. Evaluation of monotonic and non-monotonic dissipation test results. Computers And Geotechnics 2010 37: 7-8. 885-904. DOI: 10.1016/j.compgeo.2010.07.008

[17] Imre, E.: Evaluation of "short" dissipation tests. Proc. of the 12th Danube-European Conference. 2002. 499-503.

[18] Lunne, T; Robertson, P.K.; Powell, J.J.M Cone Penetration testing. Blackie Academic & Professional; 1992. 1-312.

[19] Teh, C.I. and Houlsby, G.T. Analysis of the cone penetration test by the strain path method. Proc. 6th Int. Conf. on Num. Meth. in Geomechanics, Innsbruck. 1988.

[20] Imre E, Bates L, Fityus S 2011 Evaluation of dilatometer dissipation test data with no inflexion point. In: Proc 13th International Conference of the International Association for Computer Methods and Advances in Geomechanics: IACMAG 2011. Melbourne. 2011.05.09-2011.05.11. pp. 495-501.

[21] Imre, E. Statistical evaluation of simple rheological CPT data. Proc. of XI. ECSMFE, Copenhagen, (1995). Vol. 1. 155-161.

[22] Sills, G. C Some conditions under which Biot's Equations of Consolidation Reduce to the Terzaghi's equation. Geotechnique, 1975. 251: 129-132.

[23] Baligh, M. M. Undrained deep penetration, II. pore pressures. Geotechnique, 1986. 364: 487-503.GGGG

[24] Lehane, B. M.; Jardine, R. J. Displacement-pile behaviour in a soft marine clay Canadian Geotechnical Journal. 1994. 31. 181-191.

[25] Baligh, M. M.; Levadoux, J. N. Consolidation after undrained penetration. II. Interpretation. Jl. of Geot. Eng. ASCE, 1986. 1127: 727-747.

[26] Yang, N.-C. Redriving characteristics of piles. ASCE Jl. of Soil Mech. and Found. Div. 1956.

[27] Massarch, K. R., Broms, B. B. 1977. Fracturing of Soil Caused by Pile Driving in Clay. Proc. of the 9th ICSMFE Tokyo, Vol.1. 197-200.

[28] Kármán, T. & Biot, M. A. Mathematical Meth. in Eng. McGraw-Hill. (1940).

[29] Peuchen J., Meijninger B. DrummenT 2015. Reassessment of geotechnical conditions after an offshore well incident. Proceedings of the XVI ECSMGE Geotechnical Engineering for Infrastructure and Development

[30] Imre E., Schanz T. and Vijay P. Singh (2013) Evaluation of staged oedometric tests 251-268. Proc. of the 3rd Kézdi Conference. Budapest, Hungary, 2013.05.28.ISBN 978-963-313-081-0

[31] Imre E., Schanz T., Hortobágyi Zs., Singh V.P., Fityus S. (2015) Oedometer relaxation test Proc. XVIECSMGE

[32] Imre E., Trang P.Q., Fityus S., Telekes G. A (2011) "Geomeric parameter error estimation method for inverse prolems." Proceedings of the Second International Symposium on Computational Geomechanics (ComGeo II), Cavtat, Croatia, 27-29 April, 2011.

[33] Press, W.H.; Flannery, B.P.; Teukolsky, S.A.; Wetterling, W.T. (1986): Numerical Recipes. Cambridge Univ. Press, Cambridge

Appendix 1 Consolidation model-versions

Solution in terms of m

The general solution of the models, subject to the specified boundary conditions, is the sum of two parts: one transient and one steady-state. The steady-state part of the displacement (v^p) is given by the solution of the following equation (part of the modified Equilibrium Equation):

$$E_{oed}\frac{\partial \varepsilon}{\partial r} = 0 \tag{16}$$

This is the cavity expansion model for n=2 and 3, and the K_o compression model for n=1. The solution has the following general form:

$$v^p = \frac{\alpha}{r^{n-1}} + \beta\ r \tag{17}$$

where the parameters α and β can be determined from the non-homogeneous boundary conditions.

The steady-state pore water pressure solution is the solution of the Laplacian Equation (part of the modified Continuity Equation) which is equal to zero here.

The transient solution parts for the volumetric strain (ε^t), the displacement (v^t) and the pore water pressure (u), respectively(see App 2):

$$v^t(t,r) = r^{\frac{-(n-2)}{2}} \sum_{k=1}^{\infty} C_k \left[J_{n/2}(\lambda_k r) + \mu_k Y_{n/2}(\lambda_k r) \right] e^{-[\lambda_k]^2 ct} \tag{18}$$

$$\varepsilon^t(t,r) = r^{\frac{-(n-2)}{2}} \sum_{k=1}^{\infty} C_k \lambda_k \left\{ \left[J_{(n-2)/2}(\lambda_k r) + \mu_k Y_{(n-2)/2}(\lambda_k r) \right] \right\} e^{-[\lambda_k]^2 ct} \tag{19}$$

where J_p and Y_p are the Bessel functions of the first and second kind, of order p, n is the space dimension; λ_k, μ_k are the roots of the boundary condition equations (composed from the homogeneous form of the boundary conditions); C_k (k=1...∞) are the Bessel coefficients determinable from the initial condition, and c is coefficient of consolidation ($c = k\,E_{oed}/\gamma_v$). Around 250 roots for constants λ_k, μ_k were determined for the models (see [8]).

The pore water pressure is determined from v^t by integrating the equilibrium Modified Equilibrium Equation with respect to r including boundary condition *Nr*. 1:

$$u^t = E_{oed}\int_{r_1}^{r}\frac{\partial\varepsilon^t}{\partial r} = E_{oed}\left[\varepsilon^t - \varepsilon^t(r_1)\right] \tag{20}$$

The radial effective stress at the shaft-soil interface

$$\sigma'^t_r(t,r)|_{r=r_0} = -\left[u(t,r_0) - u_{mean}(t)\right] \tag{21}$$

The total stress at the shaft-soil interface:

$$\sigma^t_r(t,r)|_{r=r_0} = u_{mean}(t) \tag{22}$$

Solution for m=1

The total stress and, the effective stress using the constitutive equation:

$$\sigma' = -\,\mathrm{E}_{\mathrm{oed}}\frac{\partial \mathrm{v}}{\partial \mathrm{y}} \tag{23}$$

and, the effective stress equality:

$$\sigma = \sigma' + u. \tag{24}$$

The total stress can be expressed with the pore water pressure and the steady-state term (underlined):

$$\sigma\ (t) = u_{mean}(t) + \underline{E_{oed}\frac{v_0}{H}} \tag{25}$$

It follows that for a realistic u the radial total stress at decreases with time by the value of the initial mean pore water pressure. The effective stress is given as:

$$\sigma'\ (t,y) = -E_{oed}\frac{\partial v\ (t,y)}{\partial y} = u_{mean}(t) - u(t,y) + \underline{E_{oed}\frac{v_0}{H}} \tag{26}$$

and, the mean effecive stress is equal to:

$$\sigma'_{mean}(t) = \underline{E_{oed}\frac{v_0}{H}}. \tag{27}$$

The steady-state displacement v^p:

$$v^p(y) = v_0\left(1 - \frac{y}{H}\right) \tag{28}$$

The transient displacement v^t for the oedometric relaxation test model:

$$v^t(t,y) = \sum_{k=1}^{\infty} a_k \cdot \sin\left(\frac{k\cdot\pi}{H}y\right)\cdot e^{-\frac{k^2\cdot\pi^2}{H^2}\cdot c_v\cdot t} \tag{29}$$

where a_k (k=1.∞) are the Fourier coefficients of an odd initial displacement function.

Function u is derived from solution v^t:

$$u(t,y) = \sum_{k=1}^{\infty}\alpha_k\left[\cos\left(\frac{k\cdot\pi}{H}y\right) - 1\right] e^{-\frac{k^2\cdot\pi^2}{H^2}\cdot c_v\cdot t} \tag{30}$$

where

$$\alpha_k = a_k\frac{k\pi}{H};\ \beta_k = -b_k\frac{k\pi}{2H}. \tag{31}$$

Only one initial condition function is to be specified (either $u_0(y)$ or $v_0(y)$), the other can be computed as follows:

$$u_0(y) = E_{oed}\frac{\partial v_0^t(y)}{\partial y} - E_{oed}\frac{\partial v_0^t(y)}{\partial y}|_{y=0}, \tag{32}$$

$$v_0^t(y) = \frac{1}{E_{oed}}\left(\int_0^y u_0(x)\,dx - y u_{0,mean}\right), \tag{33}$$

The pore water pressure solution has the following form at t=0:

$$u(0,y) = \sum_{k=1}^{\infty}\alpha_k\left[\cos\left(\frac{k\pi}{H}y\right) - 1\right] \tag{34}$$

and, the Fourier series for $u_0(y)$ has a different form:

$$u_0(y) = \sum_{k=0}^{\infty}\gamma_k\cos\left(\frac{k\pi}{H}y\right). \tag{35}$$

This problem can be eliminated, if a boundary condition is included into the initial condition:

$$\gamma_0 = -\sum_{1}^{\infty}\gamma_k \tag{36}$$

then the Fourier series for $u_0(y)$ has the same form as the solution at t=0:

$$u(0,y) = \sum_{k=1}^{\infty}\gamma_k\left[\cos\left(\frac{k\pi}{H}y\right) - 1\right] \tag{37}$$

and, in this case:

$$\alpha_k = \gamma_k, .. k > 0. \tag{38}$$

The analytical solution for the effective stress and for the total stress are as follows. The effective stress:

$$\sigma'\ (t,y) = -\sum_{k=1}^{\infty}\alpha_k\cos\left(\frac{k\pi}{H}y\right)e^{-\frac{k^2\pi^2}{H^2}c_v t} + E_{oed}\frac{v_0}{H} \tag{39}$$

The total stress s equals to the effective stress at y=0:

$$\sigma(t) = -\sum_{k=1}^{\infty}\alpha_k\ \frac{k\pi}{2H}e^{-\frac{k^2\pi^2}{H^2}c_v t} + E_{oed}\frac{v_0}{H} \tag{40}$$

Solution m=2

The function u (for the m=2, coupled 1 model):

$$u(t,r) = \sum_{k=0}^{\infty}\lambda_k C_k\, e^{-\gamma_k^2\cdot c_h\cdot t}\left\{\left[I_0(\lambda_k r) + \mu_k Y_0(\lambda_k r)\right] - \left[I_0(\lambda_k r_1) + \mu_k Y_0(\lambda_k r_1)\right]\right\} \tag{41}$$

Appendix 2 Approximate methods
Matching sigma method

The pore water pressure functions and matching data are shown in Figure 13, the measured data and the computational details are shown in Tables 14 to 17 The final total stress $\sigma_r^s(r_0)_i$ and $c_{flex}(ti)$ function and the identified c - $\sigma_r^s(r_0)_i$ functions intersect at c 2e-3 (the pore water pressure t_{50}). It can be noted that for the sigma the t_{50} is greater than the u_2 50 % dissipation time. The relation between the 50 % time for total stress and pore water pressure is not known. It can also be noted that the $\sigma_r^s(r_0)$ is negative for large t_i values.

This limit can also be considered as an empirical *cflex* time.

Flex method

The Flex method by eye gave a coefficient of consolidation range instead of a single value due to the uncertainty in the in the determination of the inflexion point. Therefore, a 3rd-order parabola was fitted, and the inflexion point was approximated where the derivative indicated a change. This method gave small *c* values and was not considered as successful.

Table 16. The piezo-lateral stress cell test data in normalized form

t_i in s	σ'_r	σ_r	u
0	0,041	1,000	0,963
20	0,041	0,988	0,947
90	0,045	0,951	0,906
190	0,049	0,918	0,865
290	0,053	0,890	0,837
490	0,057	0,853	0,792
790	0,065	0,808	0,747
1990	0,073	0,706	0,633
2990	0,078	0,653	0,571
6990	0,094	0,531	0,437
9990	0,110	0,482	0,371
19990	0,163	0,388	0,224
39990	0,233	0,314	0,086
99990	0,269	0,273	0,004

Table 17. Matching method, final stress – identified *c* relation

$\sigma_r^s(r_0)$	slow *c* in cm^2/s	fast *c* in cm^2/s
0.15	4,00E-04	1,00E-03
0.25	8,00E-04	
0.3	1,00E-03	2,00E-03
0.4	2,00E-03	3,00E-03
0.5	7,00E-03	9,00E-03

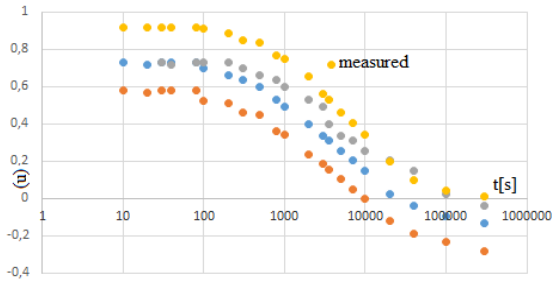

Figure 29. Matching method, generated pore water pressure functions (Tables 21 and 22).

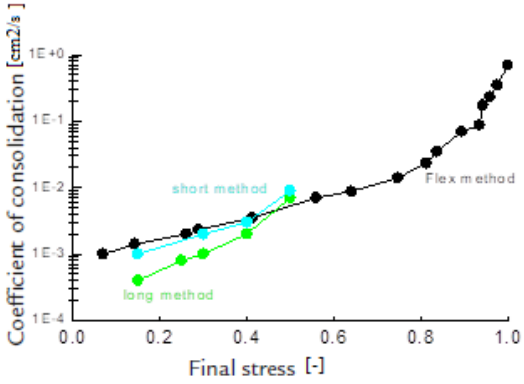

Figure 30. Matching method, final stress – identified *c* relations (Table 20)

Table 18. Assuming that $t=t_{50}$%, σ_r = sigmaflex, the computed $\sigma_r^s(r_0)$ and cflex

t_i in s	$\sigma_r^s(r_0)$	σ_r	
10	1	1	0,7
20	0,98	0,99	0,35
30	0,96	0,98	0,2333333
40	0,94	0,97	0,175
80	0,94	0,97	0,0875
100	0,89	0,95	0,07
200	0,84	0,92	0,035
300	0,81	0,91	0,0233333
500	0,75	0,87	0,014
800	0,64	0,82	0,00875
1000	0,56	0,78	0,007
2000	0,41	0,71	0,0035
3000	0,29	0,64	0,0023333
3500	0,26	0,63	0,002
5000	0,14	0,57	0,0014
7000	0,07	0,53	0,001
10000	-0,04	0,48	0,0007
20000	-0,25	0,38	0,00035
40000	-0,36	0,32	0,000175
100000	-0,42	0,29	0,00007
300000	-0,48	0,26	2,333E-05

Table 19. The *u* computation (R=relaxation term, $\sigma_{rs}(r0)$=0,15)

t_i in s	R term	σ_r-0,15	σ_r-0,15-R=$u_{0,15}$	$u_{0,15mod}$
10	0	0,85	0,85	*0,73
20	0,06	0,84	0,78	0,72
30	0,07	0,83	0,76	0,73
40	0,07	0,82	0,75	0,73
80	0,09	0,82	0,73	0,73
100	0,09	0,8	0,71	0,7
200	0,1	0,77	0,66	0,66
300	0,11	0,76	0,64	0,64
500	0,12	0,72	0,6	0,6
800	0,13	0,67	0,54	0,53
1000	0,14	0,63	0,49	0,49
2000	0,15	0,56	0,41	0,4
3000	0,16	0,49	0,34	0,34
3500	0,16	0,48	0,32	0,31
5000	0,17	0,42	0,25	0,25
7000	0,17	0,38	0,21	0,2
10000	0,18	0,33	0,15	0,15
20000	0,19	0,23	0,03	0,02
40000	0,21	0,17	-0,04	-0,04
100000	0,23	0,14	-0,09	-0,1
300000	0,25	0,11	-0,14	-0,14

Table 20. The generated *u* functions for various σ_{rs}(r0) values (see Fig. 27)

t_i in s	0,15	0,3	0,25	0,4	0,5
10	0,73	0,58	0,63	0,48	0,38
20	0,72	0,57	0,62	0,5	0,35
30	0,73	0,58	0,63	0,48	0,34
40	0,73	0,58	0,63	0,5	0,3
80	0,73	0,58	0,63	0,48	0,29
100	0,7	0,52	0,57	0,46	0,24
200	0,66	0,51	0,56	0,41	0,2
300	0,64	0,46	0,51	0,39	0,16
500	0,6	0,45	0,50	0,35	0,11
800	0,53	0,36	0,41	0,29	0,05
1000	0,49	0,34	0,39	0,24	0,02
2000	0,4	0,24	0,29	0,16	0,11
3000	0,73	0,58	0,63	0,48	0,38
3500	0,72	0,57	0,62	0,5	0,35
5000	0,73	0,58	0,63	0,48	0,34
7000	0,73	0,58	0,63	0,5	0,3
10000	0,73	0,58	0,63	0,48	0,29
20000	0,7	0,52	0,57	0,46	0,24
40000	0,66	0,51	0,56	0,41	0,2
100000	0,64	0,46	0,51	0,39	0,16
300000	0,6	0,45	0,5	0,35	0,11